

heading

Spectra of Water Sonoluminescence

authors

Y. T. Didenko* and S. P. Pugach

institutions

Pacific Oceanological Institute, Russian Academy of Sciences, Vladivostok, 690041, Russia

Received: April 7, 1994*

Content

The sonoluminescence spectra of water saturated with helium, argon, krypton, and xenon gases were studied in a 220–500 nm interval. Total light power of sonoluminescence and the yield of hydrogen peroxide increased in the order $\text{He} < \text{Ar} < \text{Kr} < \text{Xe}$. The peak position of the OH^* radical at 310 nm did not depend on the dissolved gas, but in the region $\lambda < 310$ nm the light emission had maxima at 262, 268, 250, and 242 nm for He, Ar, Kr, and Xe, respectively. The intensity of this part of the spectra increased in the same order. The results show that sonoluminescence is a kind of luminescence, and the source of sonoluminescence is not blackbody radiation or electrical discharge.

Headline

Introduction

Content

Acoustic cavitation in liquids is accompanied by a number of effects, one of which is the light emission—sonoluminescence (SL). This peculiar phenomenon has been the subject of many experimental and theoretical investigations over the past few decades (see reviews in refs 1–4), but it still remains to be poorly understood.

A few hypotheses have been proposed on the mechanism of sonoluminescence and sonochemical reactions. All of the them are based on the formation, growth, and implosive collapse of cavitation bubbles as the source of the phenomenon. Noltingk and Neppiras⁵ proposed that SL arises from blackbody emission of the adiabatic collapsed cavity. Recently, Hiller et al.,⁶ studying the spectra of water SL from a single nonlinearly pulsating cavitation bubble, suggested sonoluminescence to be blackbody radiation with temperature of heated bubble content of 25 000 K. Atchley et al.⁷ found that the temperature inside a collapsed cavity can exceed 16 200 K.

An electrical discharge inside or outside the bubble has been proposed several times for the explanation of SL⁸ (see also reviews^{1–4}).

Some researchers believed that the generation of a shock wave inside the collapsing bubble is the source of sonoluminescence,⁹ and recently it was found experimentally that SL arises when the speed of a bubble compression exceeds the speed of sound in the gas.¹⁰ However, the results of Atchley et al.^{7a,11} show that it is not necessary, and a speed of 130 m/s is enough to produce SL from a single nonlinearly pulsating cavitation bubble.

A hot-spot chemiluminescence model¹² is based on the opinion that the emission arises from active species that are formed by high temperature inside the cavitation bubble. Taylor and Jarman proposed¹³ that sonoluminescence is partly chemiluminescent in its nature and partly due to emission of heated gas.

Thus, many hypotheses have been proposed, and there is no generally accepted one.

Spectral investigations of sonoluminescence were carried out in several papers (see reviews^{1–4}). It has been shown that dissolving in liquid gases essentially changes the SL intensity and spectra.^{13–16} The spectra of SL of water saturated with oxygen, nitrogen, or their mixture are difficult to interpret because of the large number of emitting light particles, which

Content

can be formed by the chemical reactions inside the cavitation bubble.^{3,15} On the other hand, the SL spectra of noble gas-saturated water were studied insufficiently, and the interpretation of them is not still realized. This work is devoted to the studies of SL spectra of water saturated with helium, argon, krypton, and xenon gases. A preliminary report of this work has been published.¹⁷

The objectives of this paper are (i) to reconsider the possible mechanisms of sonoluminescence and (ii) to present the SL spectra of noble gas-saturated water and to interpret them. We conclude that SL is not a blackbody radiation or electrical discharge and is a kind of luminescence. The changes of SL spectra in the order of inert gases from helium to xenon are explained by the difference in noble gas characteristics and the peculiarities of the conditions inside the bubble when SL occurs.

Headline

Methods

Content

The details of experimental arrangement and procedure are presented in the previous paper.¹⁶

Distilled water was sparged with a suitable noble gas for 1 h before ultrasonic irradiation and in the course of spectra acquisition in a 0.5 L glass vessel placed in a thermostated water bath. The liquid was continuously rotated through the irradiation cell (stainless steel with cooling jacket, volume 50 cm³, inner diameter 2 cm) by using a peristaltic pump. Ultrasonic irradiation of water was carried out at 337 kHz with total absorbed power of ultrasound—15.5 W checked calorimetrically. The temperature inside the cell was controlled by a thermistor and maintained at 21 ± 0.5 °C. It was necessary from 1 to 2 h for stabilizing the transducer output and for the liquid–gas system to achieve the equilibrium, as we worked at high enough intensity of ultrasound and with the cavitation field.¹⁵ After that time the spectra were a little modified because of the instability of cavitation field dynamics. To overcome this problem, spectra were collected and averaged from 4 to 10 separate ones.

The ends of irradiation cell were fitted with the piezoceramic transducer and quartz window, respectively. The resulting sonoluminescence passed into a MDR-23 600 mm grate monochromator with the grating 1200 rulings/mm, which was blazed at 250 nm. The detector was a photomultiplier FEU-100-tube calibrated in 200–800 nm intervals. The relative response function of the detection system was determined by a 30 W deuterium lamp DDS-30 with measured spectral irradiance. Total SL light power was obtained without a monochro-

mator when the ultrasonic cell was coupled directly with the PMT tube. The resultant output of the photomultiplier was compared with that from a calibrated β -light source with known spectral irradiance which gave 3.7×10^9 photons s^{-1} in the 400–600 nm interval. We did not use D-lamp or β -light source data for the measurement of the spectral irradiance of sonoluminescence because of the big value of errors in both these cases. So SL intensity is given in Figure 1 in relative units. The total light power of SL is listed in Table 1.

Spectra were collected with 2 nm increments in the 220–500 nm interval as it is well-known that there are not any particular lines or bands in the region of the wavelengths higher than 500 nm for the SL spectra of distilled water.^{13,15} Ten measurements were acquired in each point and averaged. It was necessary around 20 min to get one spectrum. Separate spectra were smoothed by a method of successive iterations and averaged by 4–10 values.

The noise level was measured and subtracted from the spectra. The signal-to-noise ratio (S/N) depended on the SL intensity and was deteriorated with the decrease of the wavelength. The lower value of S/N was in the case of He-saturated water ≈ 20 at a maximum (310 nm) and ≈ 5 at 220 nm. However, a typical value of the signal-to-noise ratio was much higher. For example, for Ar-saturated water S/N was more than 100 at the maximum and ≈ 20 at 220 nm.

The yield of hydrogen peroxide was measured by the potassium–iodine colorimetric procedure¹⁸ after suitable time of irradiation of water in the cell with the inlet and outlet ports locked. These experiments were made simultaneously with total SL light power measurements. The initial rates of hydrogen peroxide formation were determined as the slopes of the yield (time) curves.

The number of photons emitted by the excited hydroxyl radical OH* in the 270–350 nm region was compared with the total quantity of hydroxyl radicals OH which were formed inside the individual cavitation bubble. The initial rates of hydroxyl radical formation $\omega_0(\text{OH})$ were calculated as $\omega_0(\text{OH}) = 2\omega_0(\text{H}_2\text{O}_2)$ which follows from the balance equation $\text{OH} + \text{OH} \rightarrow \text{H}_2\text{O}_2$. Thus, we assumed here that the reactions of radicals with hydrogen peroxide or others inside the bubble or in the solution after a bubble collapse are insignificant; at least they do not play a prevailing role in most cases. Actually, it is an overestimation, and this will be shown in the Discussion section. On the other hand, the number of OH* photons is evidently overestimated too because the bands of OH* species emission are superimposed in the 270–350 nm interval with the emission from other particles. Nevertheless, we guess that the OH*/OH (or, similarly, OH*/ $2[\text{H}_2\text{O}_2]$) ratio is an important parameter for studying the mechanism of sonoluminescence and sonochemistry, and the changes of it in the order of noble gases (see below) support this assumption.

Results

The spectra of sonoluminescence from noble gas-saturated water were studied in the papers,^{13,15,16} but in the work¹³ the spectra were not investigated at the wavelengths below 270 nm and in the papers^{15,16} they were not corrected with the spectral response of the detector. So the spectra presented in Figure 1 have an essentially higher intensity at $\lambda < 310$ nm than previous ones.^{13,15,16} Besides, the spectra of He-saturated water had not yet been reported, although the attempt to measure it was made in the work;¹⁵ however, the emission was too weak to observe any bands or a continuum.

The peak position of the OH* radical at 310 nm^{13,15} does not depend on the dissolved gas, but the emission from excited

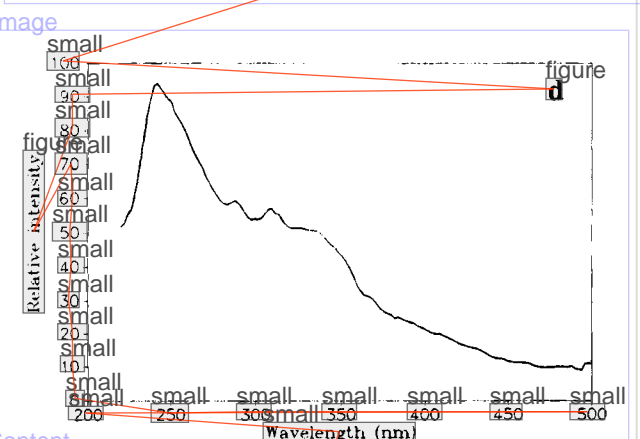
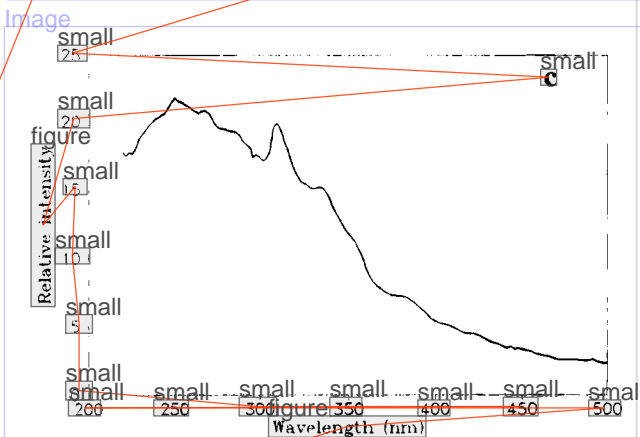
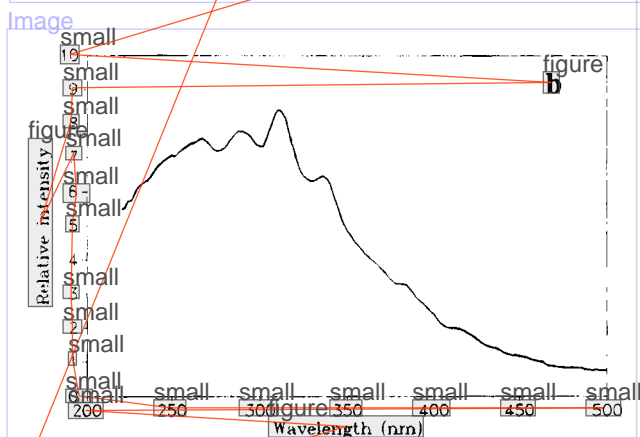
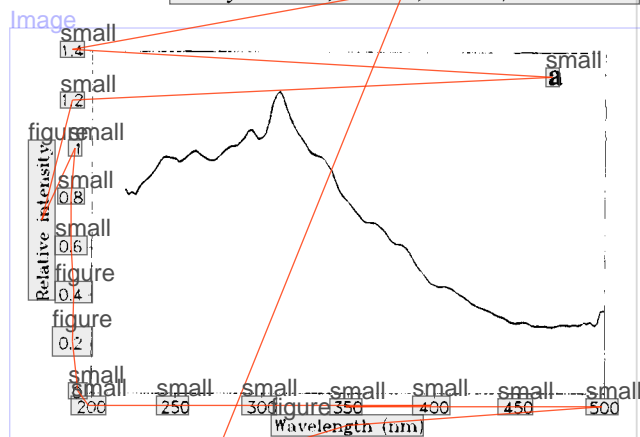


Figure 1. Sonoluminescence spectra from water saturated with helium (a), argon (b), krypton (c), and xenon (d).

H_2O^* molecule^{15,16} has maxima at 262, 268, 250, and 242 nm for He, Ar, Kr, and Xe, respectively (Figure 1). The intensity

figure

TABLE 1: Sonoluminescence and Sonochemistry Yields from Noble Gas-Saturated Water

	small gas	small xenon	figure krypton	figure argon	figure helium
total light power in 220–500 nm interval, 10^{-11} W	figure	1023 ± 36	278 ± 6	16 ± 4.2	9 ± 0.8
total number of photons in 220–500 nm interval, 10^9 units	figure	16	4.6	1.2	0.15
rate of H_2O_2 formation, 10^{-5} M min $^{-1}$	figure	1.48 ± 0.14	1.21 ± 0.12	0.79 ± 0.02	0.36 ± 0.05
number of OH* species per bubble per period, 10^3 units ^a	figure	561	170	68	53
number of OH radicals per bubble per period, 10^3 units ^a	figure	88	72	47	21
OH*/OH ratio	figure	6.4	2.4	1.1	0.26
ratio of H_2O_2 formation rate to SL intensity, relative units (from Prudhomme and Guilmar)	figure	19.6	7.5	2.51	1

^a These values are calculated for 10^4 bubbles/cm 3 .

Content

of this part of the spectra grows in the order He < Ar < Kr < Xe (Figure 1).

The total light power of SL increases in the order He < Ar < Kr < Xe (see Table 1) that is in accordance with the previously published results on the sonoluminescence intensity of noble gas-saturated water.^{19,20} The measurements of both hydrogen peroxide and sonoluminescence yields in one work were carried out also by Prudhomme and Guilmar.¹⁹ Calculated from the paper,¹⁹ the ratio of SL intensity/the yield of H_2O_2 grows in the order He < Ne < Ar < Kr < Xe, which agrees with our data: this ratio and also the OH*/OH ratio increase with increasing atomic weight of the dissolved gases from 0.26 (helium) to 6.4 (xenon) (see Table 1).

heading

Discussion

Content

There are a few hypotheses explaining the mechanism of sonoluminescence and sonochemical reactions. In principle, they can be divided into two categories: thermal, when the origin of sonoluminescence and chemical-active particles is explained by the thermal heating of a cavitation bubble content, and electrical, due to electrical discharge inside the bubble or in the surrounding liquid (see reviews^{1–4}). Electrical hypotheses were criticized and rejected,²¹ but Margulis²² proposed a new one, the essence of which is as follows.

The small size bubbles are breaking off from the bigger one that pulsates in a sound field. The neck is formed on the place of detachment, and the electrokinetic ζ -potential can concentrate there because of the flow of a charged liquid around this neck. The value of the ζ -potential is excessively great,²² so the electrical discharge can occur inside the gas phase at the time of the bubble detachment.

Note that the value of the ζ -potential decreases when the concentration of salt in the solution increases.²³ Thus, following ref 22 the SL intensity must also decrease in salt solutions. However, experimental results show an opposite dependence: sonoluminescence increases with the growth of salt concentration in salt solutions.^{24,25}

It has been shown recently²⁶ that the small additives of perfluorocarbon gases CF_4 and C_2F_6 in the mixture of Ar/ CF_4 and Ar/ C_2F_6 substantially suppress sonoluminescence. Authors²⁶ assume that these results are consistent with thermal mechanisms of SL, because these gases have low values of the ratio of specific heats $\gamma = c_p/c_v$ as compared with noble gases. Thus, the lower the value of γ , the lower cavitational temperature and the less the intensity of SL. On the other hand, CF_4 is known as an efficient gas for plasma chemistry and will support an electrical discharge. Thus, the results²⁶ are in direct contradiction with electrical discharge hypotheses and support the thermal mechanism for sonochemistry and sonoluminescence.

It was found recently^{7a,11,27} that the SL flash from the synchronously repeating stable SL, which originates from nonlinear motion of a single bubble, occurs in the final stage

Content

of its implosion. Note that the authors of the papers^{7a,11,27} were working at the intensity of ultrasound that is higher than the threshold of instability of the bubble surface, i.e., at conditions where the bubble disruption and the detachment of tiny bubbles from the bigger one seem incredible.^{7a}

The sonoluminescence spectra of hydrocarbons show no emission lines or bands of charged particles,¹⁴ which is also in disagreement with the electrical discharge hypotheses.

Nevertheless, there are no well-recognized hypotheses about the mechanism of sonoluminescence and sonochemistry, and the debates still continue.^{4,8e,f,22} To our knowledge, the majority of experimental results can be explained by the thermal hypothesis and its variations. Next we shall try to explain the data obtained in this work with the help of this hypothesis.

Sonoluminescence as Blackbody Radiation. SL occurs at the compression of a cavitation bubble just before the minimum of its size is reached.¹⁰ The velocity of the bubble wall can exceed 130 m/s¹¹ or even around the speed of sound in the gas.¹⁰ The time of SL flash is less than 50 ps, and the number of photons emitted from one flash is around 10^5 .²⁷ The spectra of SL emitted by a single cavitation bubble have a maximum at ≈ 230 nm.^{6,7} The authors of mentioned papers believe that SL is a blackbody radiation with temperature $\approx 25\,000$ ⁶ or 16 200 K.⁷ The decrease of bulk solution temperature from 22 to 10 °C increases a blackbody temperature to 50 000 K.⁶

Suppose that sonoluminescence is the equilibrium thermal radiation at 25 000 K. Let us estimate the number of photons emitted by a single bubble. The SL flash occurs at the bubble radius $R_{SL} \approx 2.2 \times 10^{-4}$ cm.¹⁰ The density of the bubble content at its minimum size should be around liquid density.¹³ Thus, the number of particles inside the bubble N_0 at $R = R_{SL}$ is about $N_0 \approx 10^{12}$. The number of particles N_i with the energy of $\epsilon_i \approx 5.4$ eV ($\lambda \approx 230$ nm, maximum in the spectra^{6,7}) is, in accordance with the Boltzmann distribution, $N_i \approx N_0 \exp(-\epsilon_i/kT) \approx 7 \times 10^{10}$. The experimentally determined value of N_i is $\approx 10^5$.²⁷ So, at equilibrium temperature of 25 000 K the number of photons emitted by one cavitation bubble must be 5 orders larger than the experimental value. For N_i to be equal to the calculated value, temperature inside the bubble has to be around 4000–4500 K. However, in this case according to Wein's rule, the maximum in the spectra has to be situated in the region of 725–644 nm. Thus, the temperature inside the bubble cannot be so high (25 000 K or even 50 000 K⁶), and it is probably around the values estimated in refs 28 and 29.

The calculations of temperature from the experimental data on the broadening of potassium lines²⁸ or on the rovibrational distribution of the lines in the C_2^* band²⁹ gave the values of 3360 ± 330 and 5075 ± 156 K, respectively. The temperature inside the bubble is distributed irregularly: its maximum in the center can be 5-fold higher than average one.³⁰ For example, according to ref 31, the liquid temperature around the bubble does not differ essentially from that in the bulk liquid; however, the temperature on the bubble–liquid frontier from the bubble side can be ≈ 1900 K and in the bubble center ≈ 5200 K.

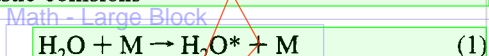
At the average temperature inside the bubble of $T = 5000$ K, the number of molecules with $\epsilon_i = 10$ eV (the energy of the first stable excited state \tilde{C}^1B_1 of water molecule³²), N_i , is ≈ 14 ; at $T = 8000$ K $N_i \approx 1.7 \times 10^5$. The number of molecules with $\epsilon_i = 8.3$ eV (the energy of \tilde{B}^1A_1 state³²), N_i , is $\approx 10^3$ at $T = 5000$ K and $N_i \approx 4 \times 10^5$ at $T = 7000$ K. Thus, the average temperature inside the bubble at the conditions of refs 6 and 7b is, probably, within the 5000–8000 K limits.

The time of SL flash is very short, $\approx 10^{-10}$ s.²⁷ Atoms and molecules can take part in 10^3 collisions in this time.¹³ Consequently, the equilibrium can be achieved only for the translational degrees of freedom, partly for dissociation and electronic, rotational, and vibrational transitions. The ionization and ionic recombination processes are far from the equilibrium.¹³ Probably, more correctly, one should discuss the “effective” temperature inside the bubble.²⁹ Hence, we shall mean the effective temperature inside the bubble in discussing the results obtained in this work.

The luminescent nature of SL has been repeatedly proved so the supposition that sonoluminescence has to be blackbody radiation needs addition argumentations. Probably, this conclusion has been made by the authors of refs 6 and 7 because they did not detect any lines or bands in the spectra. Actually, SL was obtained from the bubble, which contains air gases and water vapors. These spectra are broadened; the band from the excited OH^* radical is not prominent^{13,15} because of the luminescence of the products of the chemical reactions of nitrogen and oxygen atoms and molecules inside the cavitation bubble.^{2,15}

The results of recently published papers on the spectra of SL of organic liquids¹⁴ are in contradiction with the blackbody mechanism.⁶ Those spectra show a prominent emission from the excited C_2^* radical.¹⁴ The SL spectra of dodecane were studied in the presence of He, Ne, and Ar and in the mixture of He/Ar. The data showed that the ratio of the intensity of C_2^* emission to the intensity of a continuum does not depend on the thermal conductivity of the dissolved gas. Besides, no bands or lines were detected in those spectra at wavelengths shorter than 300 nm.¹⁴ Thus, one can conclude that the bands at $\lambda < 270$ nm in the SL spectra of water saturated with noble gases (Figure 1) are not the emission of the heated gas. Otherwise, they must be presented in the spectra of ref 14. Thus, these bands originate from the emission of water molecules or some particles which contain a water molecule (or the product of its dissociation) with the atoms of noble gases. It is very difficult also to explain with the help of the blackbody mechanism of sonoluminescence the very short time of SL flash and the fact that it is over before the minimum size of a bubble is reached.¹⁰ Thus, the blackbody mechanism of SL is inconsistent with the experimental results.

Interpretation of Spectra. The compression of a cavitation bubble starts slowly, almost isothermally. Vapors are partly condensed, and the evolved heat of condensation is extracted by the thermal conductivity of a liquid. Next, the velocity of a bubble compression increases, and it shrinks almost adiabatically with the continuous growth of temperature and pressure. The kinetic energy of particles inside the bubble also increases. It can be converted into the energy of electronic excitation by means of inelastic collisions^{3,15}

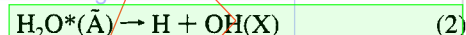


where M is the atom of a gas or a water molecule. As a result of reaction 1, the singlet-excited water molecules are formed.¹⁶ The supposition on the formation of triplet-excited water molecules $H_2O^*(^3B_1)$ ¹⁵ is doubtful as the singlet–triplet transi-

Content

tions have a low probability; in addition, they usually need more time ($> 10^{-3}$ s) as compared with the singlet–singlet transitions ($\approx 10^{-12}$ – 10^{-8} s).

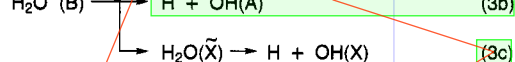
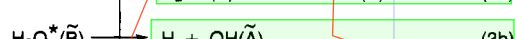
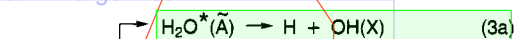
A small energy of excitation (≈ 7.5 eV) can lead to the first singlet-excited state of water molecule, \tilde{A}^1B_1 .³² This state is repulsive, and the water molecule dissociates into hydrogen atoms and hydroxyl radicals in a quiescent electronic state.³²



Content

At energies of excitation greater than 8.3 eV ($\lambda < 150$ nm) the \tilde{B}^1A_1 excited state of water molecules is reached.³² This state is less repulsive, and the dissociation gives the electronic excited radicals $OH^*(^2\Sigma^+)$.³²

Math - Large Block



Content

The yield of $H_2O(\tilde{B})$ molecules is less than 10%, and 90% of them dissociate by processes 3a–3c.³² If the energy transmitted by the collision (1) is as high as 9.9 eV, then water molecules excite on the stable singlet \tilde{C}^1B_1 state.³² The formed water molecule $H_2O(\tilde{C})$ can lose the excess energy either through the $H_2O(\tilde{B})$ state followed by reactions 3a–3c or by the light emission at $\tilde{C} \rightarrow \tilde{A}$ transition.³²

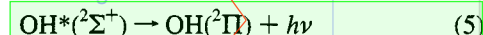
Math - Large Block



Content

The $\tilde{C} \rightarrow \tilde{A}$ transition is accompanied by the broad-band emission in the region from 380 to 600 nm with the maximum at 425 nm.³² Excited radical $OH^*(^2\Sigma^+)$, formed by reaction 3a, emits light at 280, 310, and 340 nm in the spectra of SL following the $1 \rightarrow 0$, $0 \rightarrow 0$, $0 \rightarrow 1$ transitions.^{13,15}

Math - Large Block

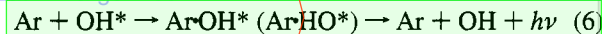


Content

Sonoluminescence occurs at the final stage of a cavitation bubble compression, with the high pressure inside it. Thus, one can suppose the formation of excimer molecules like $(M\cdot OH)^*$, M_2^* , and $(M\cdot H_2O)^*$.

The decomposition of the $Ar\cdot OH^*$ excimer is accompanied by the emission at 310, 316, and 318 nm and of $Ar\cdot HO^*$ (excimer) at 340 nm.³³

Math - Large Block

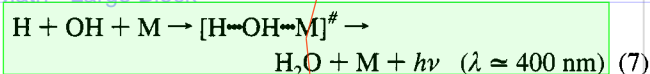


Content

Thus, these particles can contribute to the light emission of the spectra of water sonoluminescence.

The continuum of the spectra originates from the radiative stabilization of a quasimolecule formed by the reaction^{15,34}

Math - Large Block



Content

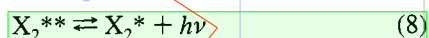
where $\#$ denotes the vibrational excited complex molecule.

Consider the possible addition to the SL spectra of the excited atoms and molecules of noble gases. The M_2^* excimers radiate in broad-band emission with the maximum in the ultraviolet field. This maximum shifts to a short-wave region with the decrease in atomic weight of a gas. For example, the maximum is situated at 170 nm for xenon and at 126 nm for argon.³⁵ The bands at 195 nm (Ar), 220 nm (Kr), and 300 nm (Xe) originate from the reaction of ion–electron recombination like $X^+ + e^-$

Content

→ X^{**} or $X^+ + e^- \rightarrow X^*(^3P_{1,2})$.³⁵ Such prominent bands in the SL spectra of noble gas-saturated water were not discovered (see Figure 1 and refs 13, 15, and 16). This supports, in our mind, the opinion that electrical phenomena are not major in the mechanism of a cavitation light emission.

The continuum in the near-ultraviolet field with the maximum at 210 nm (Ar) or 270 nm (Kr) is formed by the transitions³⁶



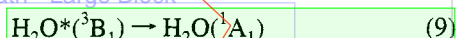
Content

Note that the maximum of the emission shifts to a longer wave region with the increase in atomic weight of noble gas. Thus, it is impossible to explain the results of Figure 1 by reaction 8 as we observed an opposite dependence: the maxima in the spectra are shifted to the short-wave field with the increase in atomic weight of noble gas (Figure 1).

The lines of noble gas in the spectra of SL were not also discovered before.^{13,15,16} This can be a consequence of two causes. First, the excitation energy of noble gases is higher than that one of water; thus, the temperature inside the cavitation bubble is not high enough for the formation of excited molecules or atoms of noble gases. Second, water molecules quench effectively the excited states of noble gas atoms.³⁷

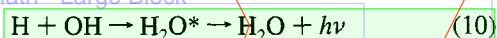
Thus, the continuum in the spectra is formed by fast transition ($\approx 10^{-12}$ s³²) $\tilde{C}^1B_1 \rightarrow \tilde{A}^1B_1$ (reaction 4b) and by the recombination (7). Note that the vibrational excited water molecules can also be formed by reaction 1.

It is still not clear what kind of species emits the light at wavelengths below 310 nm. Sehgal et al.¹⁵ believe that this emission occurs by the transition



Content

In addition, they write that "...The short wavelength cutoff at 235–245 nm or 113–117 kkal/mole gives the heat of reaction $H_2O \rightarrow H + OH$ (all in the ground state) at 0 K in good agreement with the thermal value of 119 kkal/mole".¹⁵ Probably, authors of that paper assumed that the emission originates by two-body collision with the radiative stabilization of the product:



Content

Unfortunately, the details of this reaction are not described. Really, two-body collisions in the conditions of high pressure inside the bubble, when SL originates, have much lower probability than three-body collisions like (7). The formation of triplet-excited water molecule is doubtful (see above). In addition, the excitation energy of the $H_2O^*(^3B_1)$ molecule is 7.1 eV;³⁸ consequently, the emission at the transition (9) has to be at $\lambda > 175$ nm (7.1 eV), and the shift of the maximum to 280 nm¹⁵ is difficult to explain. Thus, the position of the emission maxima at $\lambda < 300$ nm in SL spectra (Figure 1) cannot be explained by reactions 9 and 10.

The transition from the excited \tilde{B} or \tilde{C} states of water molecule to the quiescent state has to be accompanied by the vacuum-ultraviolet emission as the excitation energy of these states is ≈ 8.3 and 10 eV, respectively.³² Really, the maximum in the SL spectra of noble gas-saturated water is situated at 262, 268, 250, and 242 nm for He, Ar, Kr, and Xe, respectively, and the intensity of those bands increases in the same order (Figure 1). One could assume that SL is blackbody radiation; then both these experimental observations can easily be explained by the increase of temperatures inside the cavitation bubble in the order from He to Xe followed by the decrease of thermal conductivity in the same order.³⁹ However, SL is not

Content

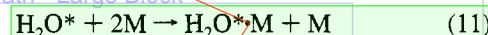
a blackbody radiation, the band at $\lambda < 300$ nm is not formed by the noble gas emission (see above), and a water molecule dissociates at high temperature, giving the excited $OH^*(^2\Sigma^+)$ radical which emits at 310 nm.

Thus, it is impossible to explain the results obtained in this paper with the help of known data on the emission of excited water molecules or excited atoms of the inert gases. We propose that the bands at $\lambda < 300$ nm in the spectra of water SL are due to the emission of excimer molecules like $H_2O^* \cdot M$.

It is well-known that noble gases can form complexes with water molecules and their stability increases in the order from argon to xenon.⁴⁰ The pressures of dissociation of Ar, Kr, and Xe hydrates at 0 °C are 105, 14.5, and 1.45 atm, respectively. The increase of static pressure promotes the growth of clusters concentration.⁴¹ Thus, one can say that the clusters like $mH_2O \cdot nM$, where $m, n = 1, 2, 3$, etc., and M is the atom of a gas, can be formed after bubble collapse and cooling. On the other hand, at the process of bubble collapse, when temperature inside it is increasing, the formation of big clusters seems less probable. So we can only propose that the excimers and clusters like $H_2O^* \cdot Xe$ and $H_2O \cdot Xe$ can be formed at the conditions of a bubble collapse.

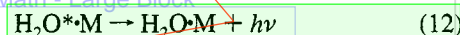
The dissociation energy D_e of such van der Waals complexes is not high. For example, D_e of ArH_2O molecule is around 0.02 eV.⁴² Similar weak bounded complexes exist, and they are described in the literature (see review in ref 43).

The excimers are formed by three-body collisions:



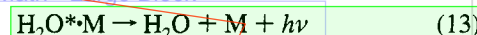
Content

This process takes place at short distances between H_2O^* and M, where the collisional potential is higher or around thermal energy, because only in this case a third particle can remove the excess kinetic energy of H_2O^* and M.⁴³ The quiescent state for for these excimers can be bounded



Content

or unbounded

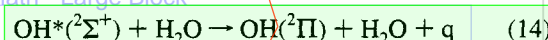


Content

The distance between H_2O^* and M will increase in the order of Ar-, Kr-, and Xe-containing excimers following the increase in atomic shell size. Thus, the energy difference between excited and quiescent states will increase, but the wavelength of emission will decrease in the same order, which was detected in the experiments (Figure 1). A similar relationship was revealed in the order of weakly bounded excimers $KrXeF^*$, $KrXeCl^*$, $KrXeBr^*$, and $KrXeI^*$.⁴³

Note that the formation of excimers like $H_2O^* \cdot N_2$ and $H_2O^* \cdot O_2$ inside the cavitation bubble is also possible as the corresponding clusters exist.^{40,41} Probably, the band discovered in refs 6 and 7 around 230 nm originates from these species.

Formed as a result of reaction 1, the excited water molecule can react by processes 3, 4, and 11 or with the unexcited water molecules, the concentration of which inside the cavitation bubble is high enough (see above). In the last case the energy can transform very effectively ("resonant quenching"). In addition, water molecules quench the excited states of hydroxyl radical³⁷



Content

Thus, the total scheme (simplified of course) of chemical reactions inside the cavitation bubble, which lead to SL, in the presence of noble gas can be presented as follows:

formation of OH radicals is the destruction of water molecules by reactions 1–4. At higher temperatures reaction 23 plays a dominant role and produces an additional quantity of OH radicals.⁴⁷ There were considered 21 chemical reactions influencing the yield of OH radicals inside the cavitation bubble at the time of its implosion. Unfortunately, the mechanism of the excited species reactions inside the cavitation bubble was not considered in ref 47.

Thus, the mechanism of formation and chemical reactions of excited particles and radicals is very complex, and it can change depending on the conditions inside the bubble at the time of its compression. We did not consider in detail all the possible processes as, first, the mechanism of reactions and the type of the species formed are not clear, and, second, the calculation of temperature inside the bubble at high amplitude of its pulsation is complicated.⁴⁷

Effect of Noble Gas Properties. Since the time when it was first discovered by Prudhomme and Guilmar,¹⁹ a number of papers were devoted to the studies of the noble gas properties on the yield of hydrogen peroxide and sonoluminescence. A principal conclusion has been made by Hickling³⁹ and was confirmed by others researchers,²⁰ that the major reason of the increase of SL and the yield of H₂O₂ is the decrease of thermal conductivity of a gas in the order of noble gases He > Ne > Ar > Kr > Xe. As a result of this, the temperature inside almost adiabatically collapsing cavitation bubble increases in the same order.

The solubility of a gas can also have an influence on SL and on the yield of hydrogen peroxide. Actually, the increase of a gas solubility in the order from He to Xe is accompanied by the growth of the number of emitting light bubbles and, thus, by the increase of SL and the yield of H₂O₂.

However, this cannot explain the changes in SL spectra and in the OH*/OH ratio in the order of noble gases. Following the scheme of eq 15, these changes can be the result of SL quenching as a consequence of different vapor/gas ratio inside the cavitation bubble filled by different noble gas. Actually, the increase of gas solubility from He to Xe promotes the process of a gas diffusion into the bubble as it expands, but the diffusivity of noble gases decreases in the same direction and seems to offset the growth of the bubble.³⁹ Studying SL from a single nonlinearly pulsating cavitation bubble, the authors of ref 7b found the variation of the SL intensity with time. This can be due to the processes of the gas diffusion inside and outside the bubble. In a cavitation field the processes of rectified diffusion are complicated by the translational motion and coagulation of bubbles. Thus, the effects of a gas solubility on the vapor/gas ratio inside the cavitation bubble need more detailed experimental and theoretical examinations.

The changes of thermal conductivity of gas can also change the vapor/gas ratio inside the bubble. In the stage of a bubble expansion the temperature of liquid–gas interface decreases because of the evaporation of water into the bubble. Thermal diffusivity of the gas contained inside the bubble corrects this deviation from the bulk solution temperature. So, the temperature on the bubble wall adjacent to the gas phase and the vapor pressure inside the bubble will be higher in the case of the gas with higher thermal diffusivity; that is, it will grow in the order from Xe to He. However, the temperature drop on the bubble–liquid interface is small and becomes significant only at high enough temperatures⁴⁸ of a bulk solution. Actually, thermal processes occur at the bubble growth in dynamics, when crispation appears on a bubble surface and the diffusion of a gas inside the bubble can influence the rate of evaporation. Thus,

Content

from this point of view we cannot make any definite conclusion about the vapor–gas ratio inside the bubble at the stage of its expansion.

Thermal conductivity of a gas plays a significant role in the vapor/gas ratio also at the time of the bubble collapse: the higher the thermal conductivity, the smaller the radius and the higher the pressure inside the bubble.⁴⁹ Assume that the vapor pressure inside the bubble at the stage of its maximal size is equal for all noble gases, filling the bubble, then at the stage of the minimal bubble size the vapor pressure will increase in the order Xe < Kr < Ar < He-filled vapor–gas cavitation bubble.

Thus, the solubility and the thermal conductivity of noble gas can, in principle, influence the gas/vapor ratio inside the cavitation bubble. However, it is difficult to estimate the significance of these effects at this time.

The results obtained in this work can be simply explained by assuming that the temperature inside cavitation bubbles increases in the order He < Ar < Kr < Xe following the decrease in thermal conductivity.³⁹ Thus, the yields of SL and hydrogen peroxide also increase in the same order.

The temperature inside the He-containing bubble is not high enough to produce the large quantity of water molecules in the \tilde{C} state, and the \tilde{A} and \tilde{B} states are generally formed. The dissociation of these states is accompanied basically by OH radical formation in a quiescent electronic state (reactions 2, 3a, and 3c). The number of water molecule in the \tilde{B} state is lower than in the \tilde{A} state so the ratio of OH*/OH is small, ≈ 0.26 (Table 1).

The growth of temperature inside the bubble promotes the number of water molecules in \tilde{B} and \tilde{C} states. As a result, the ratio of OH*/OH and the short-wave part of the spectra of $\lambda < 270$ nm increase in the order He, Ar, Kr, Xe (Table 1 and Figure 1).

Conclusions

Sonoluminescence originates from the thermal heating of the cavitation bubble content at the final stage of its compression. The unexpectedly high velocity of the SL decay cannot be explained by thermal losses.⁴⁷ Besides that SL is over before the minimum size of a bubble is achieved, but following to thermal theory the temperature inside the bubble must be maximal at that moment. Thus, SL is not a blackbody radiation and is a form of luminescence. The concentration of excited particles inside the bubble is small, but the density of its content is high, so the processes of luminescence quenching can be very effective and they determine the SL (time) dependence.

The obtained experimental results can be easily explained by the decrease of thermal conductivity and, consequently, by the increase of temperature inside collapsing cavitation bubble in the order of noble gases from He to Xe. Correspondingly, the number of water molecules excited on higher electronic states also increases. Thus, the SL intensity, the yield of hydrogen peroxide, and the OH*/OH ratio increase in the same order.

It is difficult to estimate quantitatively the processes inside the bubble as the temperature calculations at high amplitude of the bubble pulsations are complicated. In addition, the conditions inside the collapsing cavitation bubble are very peculiar to use directly the results from other fields of physics and chemistry. In this paper an attempt to describe the mechanism of SL was made, which could explain qualitatively the main points of the observed phenomena.

References

References and Notes

- (1) Walton, A. J.; Reynolds, G. T. *Adv. Phys.* **1984**, *33*, 595.

references

- (2) Verrall, R. E.; Sehgal, C. Sonoluminescence. In *Ultrasound: Its Chemical, Physical and Biological Effects*; Suslick, K. S., Ed.; VCH Publishers: New York, 1988; pp 227-286.
- (3) Margulis, M. A. *Sov. Phys.-Acoust. (Engl. Transl.)* **1969**, *15*, 153.
- (4) Suslick, K. S.; Doctycz, S. J.; Flint, E. B. *Ultrasonics* **1990**, *28*, 1280.
- (5) Nolting, B. E.; Neppiras, E. A. *Proc. Phys. Soc.* **1950**, *63B*, 674.
- (6) Hiller, R.; Putterman, S. J.; Barber, B. P. *Phys. Rev. Lett.* **1992**, *69*, 1182.
- (7) (a) Atchley, A. A. *Advances in Nonlinear Acoustics*; Hobak, H., Ed.; World Scientific Publishers: London, 1993; p 36. (b) Carlson, J. T.; Lewia, S. D.; Atchley, A. A.; Gaitan, F. D.; Maruyama, X. K.; Lowry, M. E.; Morano, M. J.; Sweider, D. E. In ref 7a, p 406.
- (8) (a) Harvey, E. N. *J. Am. Chem. Soc.* **1939**, *61*, 2392. (b) Frenkel, Y. I. *Russ. J. Phys. Chem.* **1940**, *14*, 305. (c) Degrois, M.; Baldo, P. *Ultrasonics* **1974**, *14*, 25. (d) Margulis, M. A. *Ultrasonics* **1985**, *23*, 157. (e) Lepoint, T. *Abstracts of the Third Meeting of the ESS, March 28-1, April 1993*; Figueira da Foz, Portugal, 17. (f) Margulis, M. A. *Ultrasonics* **1992**, *30*, 452.
- (9) (a) Jarman, P. D. *J. Acoust. Soc. Am.* **1960**, *32*, 1459. (b) Vaughan, P. W.; Leeman, S. *Acustica* **1986**, *59*, 279.
- (10) Barber, B. P.; Putterman, S. J. *Phys. Rev. Lett.* **1992**, *69*, 26, 3839.
- (11) Lentz, W. L.; Atchley, A. A.; Gaitan, F. D.; Maruyama, X. D. In ref 7, p 400.
- (12) Fitzgerald, M. E.; Griffing, V.; Sullivan, J. J. *Chem. Phys.* **1956**, *25*, 926.
- (13) Taylor, K. J.; Jarman, P. D. *Aust. J. Phys.* **1970**, *23*, 319.
- (14) Flint, E. B.; Suslick, K. S. *J. Am. Chem. Soc.* **1989**, *111*, 18, 6987.
- (15) Sehgal, C.; Sutherland, R. G.; Verrall, R. E. *J. Phys. Chem.* **1980**, *84*, 388.
- (16) Didenko, Y. T.; Gordeychuk, T. V.; Koretz, V. L. *J. Sound Vibr.* **1991**, *147*, 3, 409.
- (17) Didenko, Y. T.; Pugach, S. P. *Ultrasonics-Sonochemistry*, **1994**, *1*, 59.
- (18) Mead, E. L.; Sutherland, R. G.; Verrall, R. E. *Can. J. Chem.* **1976**, *54*, 114.
- (19) Prudhomme, R. O.; Guilmar, Th. *J. Chim. Phys.* **1957**, *54*, 336.
- (20) (a) Young, F. R. *J. Acoust. Soc. Am.* **1976**, *60*, 100. (b) Ciuti, P.; Iannetti, G.; Tomasini, F. *Acustica* **1991**, *73*, 277.
- (21) (a) Sehgal, C. M.; Verrall, R. E. *Ultrasonics* **1982**, *22*, 37. (b) Margulis, M. A. *Russ. J. Phys. Chem.* **1981**, *55*, 154.
- (22) Margulis, M. A. *Ultrasonics* **1985**, *23*, 157.
- (23) Antropov, L. I. *Theoretical Elektrochemistry* (Russian); Vishayashkola: Moscow, 1984.

References

- (24) Dezhkunov, N. V.; Iernetti, G.; Prokhorenko, P. P.; Franchescutto, A.; Ciuti, P. *Ing.-Fiz. Zh. (Rus.)* **1986**, *51*, 417.
- (25) Flint, E. B.; Suslick, K. S. *J. Phys. Chem.* **1991**, *95*, 1484.
- (26) Suslick, K. S.; Kemper, K. A. *Ultrasonics* **1993**, *31*, 463.
- (27) Barber, B. P.; Hiller, R.; Arisaka, K.; Fetterman, H.; Putterman, S. *J. Acoust. Soc. Am.* **1992**, *91*, 3061.
- (28) Sehgal, C.; Steer, R. P.; Sutherland, R. G.; Verrall, R. E. *J. Chem. Phys.* **1979**, *70*, 2242.
- (29) Engel, V.; Suslick, K. S. *Science* **1991**, *253*, 1397.
- (30) Margulis, M. A. *Sov. Phys-Acoust. (Engl. Transl.)* **1975**, *21*, 760.
- (31) Suslick, K. S.; Hammerton, D. A.; Cline, R. C. *J. Am. Chem. Soc.* **1985**, *107*, 5641.
- (32) Engel, V.; Meijer, G.; Bath, A.; Andersen, P.; Schinke, R. *J. Chem. Phys.* **1987**, *87*, 4310.
- (33) Lemair, J. L.; Tchang-Brillet, W.-U. L.; Shafizadeh, N.; Rostas, F.; Rostas, J. *Chem. Phys.* **1989**, *91*, 6657.
- (34) Sakuma, T. K.; Nyborg, W. L. *J. Chem. Phys.* **1970**, *53*, 1722.
- (35) Koehler, H. A.; Ferderberger, L. J.; Redhead, D. L.; Ebert, P. J. *Phys. Rev. A* **1974**, *9*, 768.
- (36) Birot, A.; Brunet, H.; Galy, J.; Millet, P.; Teyssier, J. L. *J. Chem. Phys.* **1975**, *63*, 1469.
- (37) Kondratiev, V. N.; Nikitin, E. E. *The Kinetics and Mechanism of Gas-Phase Reactions*; Nauka: Moscow, 1974.
- (38) Hertzberg, G. *Electronic Spectra and Electronic Structure of Polyatomic Molecules*; Toronto 1966.
- (39) Hickling, R. *J. Acoust. Soc. Am.* **1963**, *35*, 967.
- (40) Remi, G. *Lehrbuch der anorganischen chemie B.1*; Leipzig, 1960.
- (41) Laque, T.; Kotake, S. *J. Chem. Phys.* **1989**, *91*, 162.
- (42) Nusselt, D. J.; Lascoba, R. *J. Chem. Phys.* **1992**, *97*, 8096.
- (43) Smirnov, B. M. *Usp. Fiz. Nauk* **1983**, *139*, 53.
- (44) Pikaev, A. K.; Kabakchi, C. A. *The Reaction Ability of Primary Products of Water Radiolysis* (Russian); Energoizdat: Moscow, 1982.
- (45) Fisher, C.-H.; Hart, E. J.; Henglein, A. *J. Phys. Chem.* **1986**, *90*, 222.
- (46) Anbar, M.; Pecht, I. *J. Phys. Chem.* **1967**, *71*, 1246.
- (47) Kamath, V.; Prosperetti, A.; Egolfopoulos, F. N. *J. Acoust. Soc. Am.* **1993**, *94*, 248.
- (48) Plesset, M. S.; Prosperetti, A. *Annu. Rev. Fluid Mech.* **1977**, *9*, 145.
- (49) Flynn, H. G. *Physics of Acoustic Cavitation in Liquids*. In *Physical Acoustics*; Mason, W. P., Ed.; Academic Press: New York, 1964.